14th IMEKO TC10 Workshop Technical Diagnostics
New Perspectives in Measurements, Tools and Techniques
for system's reliability, maintainability and safety
Milan, Italy, June 27-28, 2016

The control system of primary oscillation for micromechanical gyroscope

P. Baranov, T. Nesterenko, E. Tsimbalist, E. Barbin, A. Koleda, S. Vtorushin

National Research Tomsk Polytechnic University, Tomsk, Russia
e-mail: [bpf, ntg, tsimbalist, zill130, kopranchikos, vtorushin]@tpu.ru

***Abstract* – The mode of primary oscillations of micromechanical gyroscopes sensor is provided by the electrostatic comb-drive actuator in which the interaction between the micromechanical structures and electronics occurs by means of a single or differential capacitive sensors. The paper presents a new approach to the primary oscillation control system of the two-component micromechanical gyroscope. The method of calculating natural resonant frequency is based on measurements of the total current passing through the comb-driver actuator capacitances and the lock-in detection is suggested.**

I. INTRODUCTION

Micromechanical gyroscopes (MMG) have a vibrating structure based on the energy transmission at an angular rate of rotation of the gyroscope's support frame between two normal directions (primary oscillation and secondary oscillation channels) [1–3]. MMG includes two subsystems, namely: electromechanical sensor represented by a silicon structure with movable electrodes; stationary electrodes connected with the glass support; and the electronic subsystem depending on such MMG properties as operable time upon its actuation, ratios of the angular rate transformation into the output signal and their stability at disturbing factors, conversion errors.

The mode of primary oscillations of MMG sensor is provided by the electrostatic comb-drive actuator in which the interaction between the micromechanical structures and electronics occurs by means of a single or differential capacitive sensors. With MMG power on, the sensor exposed to electrostatic forces in gaps between the comb electrodes, reciprocates along the selected axis at frequency close to that of the excitation source.

The general structure of the primary oscillation control system can be conventionally divided into two parts. The first is the excitation force shaper of sensor represented by an electrostatic actuator. The second is the parameter control system of the inertial mass primary oscillations that provides the amplitude and frequency stabilization, since the relevant data on sensitive axes are proportional, due to Coriolis forces, not only to the angular rates but also the amplitude of primary oscillations [4–6].

The maximum vibrational amplitude of mechanical vibrating system or MMG sensor subjected to the periodic force, is achieved at coincidence of its excitation and resonant frequencies. Micromechanical gyroscopes are very sensitive to temperature changes [7–9]. Hence, changes are observed in resonance frequencies and tuning of the primary oscillation channel and the scaling factor. Thus, at disturbing factors, the primary oscillation control system must provide and maintain the value trimming resulting in the simultaneous stabilization in frequency and amplitude of primary oscillations [10-11].

II. GYROSCOPE STRUCTURES

The authors suggest a new approach to the primary oscillation control system of the two-component micromechanical gyroscope with decoupling frames (Fig. 1). The sensor comprises frame 1 which executes primary oscillations together with decoupling frames 2 and 3 along *X*-axis. Comb electrodes with capacitances *C*1 and *C*2 excite primary oscillations. Differential capacitances *C*6 and *C*7 can be used to retrieve data on primary oscillation. At the angular rate Ω_z and Coriolis force, the decoupling frame 2 executes secondary (sensor) oscillations along *Y*-axis and transfers them to inertial mass 4. The angular rate Ω_y induces oscillations of inertial mass 5 through the decoupling frame 3 along *Z*-axis. Capacitances *C*3, *C*4, *C*5 are capacitive sensors of the signal processing system for angular rates Ω_z and Ω_y.

The micromechanical gyroscope sensor is implemented in its design shown in Fig. 2. For creation MMG is very important to perform the proximity natural frequencies primary and secondary oscillations of axes.

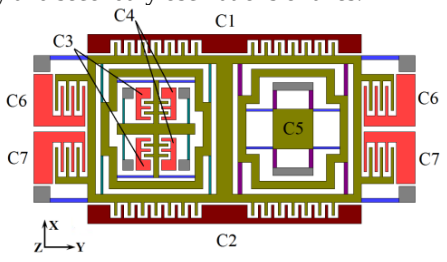

1 – frame; 2, 3 – decoupling frames; 4, 5 – inertial masses.

Fig. 1. Function circuit of MMG sensor:

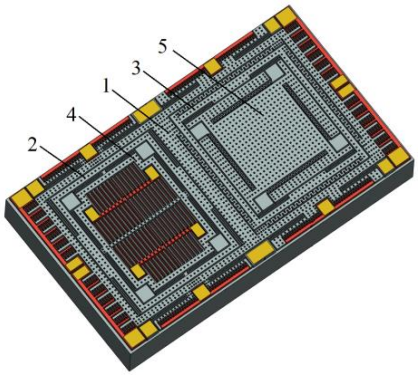

Fig. 2. Schematic drawing of silicon sensor

The results of modal analysis of the MMG are shown in Fig. 3, 4 and 5.

The modal analysis shows that the sensor elements oscillate along the axes of the primary and secondary oscillations with close frequencies.

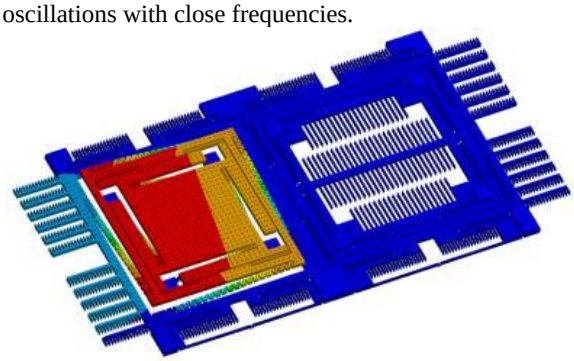

Fig. 3. 1st own mode of MMG sensor oscillations (fz = 9996,6 Hz)

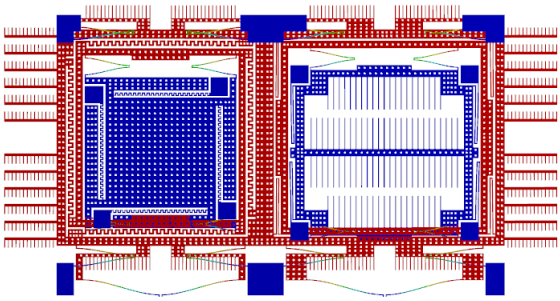

Fig. 4. 2nd own mode of MMG sensor oscillations (fx = 10015 Hz)

III. THE ANALYSIS OF PRIMARY OSCILLATION CHANNEL

Traditionally, two groups of the comb capacitor structures are used to provide the mode of primary oscillations and their stabilization in MMG sensor [12–17].

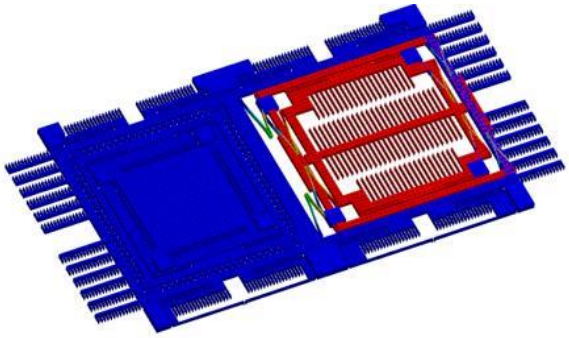

Fig. 5. 3rd own mode of MMG sensor oscillations (fy =10017 Гц Hz)

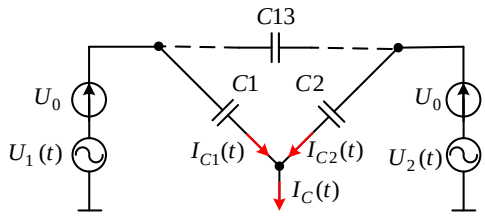

Fig. 6. Schematic of balance actuator of MMG sensor

The first group implies comb electrodes with capacitances $C1$ and $C2$ that excite primary oscillations (Fig. 1). The second group implies drive feedback electrodes with differential capacitances $C6$ and $C7$ that are used to retrieve data on primary oscillations for their further control and stabilization. With this view, the structural optimization of the comb-drive actuator results in the use of only the first group of capacitances $C1$ and $C2$ that will be the elements of the comb-drive actuator of sensor and perform measuring functions. Actually, owing to the mechanical movement of MMG sensor, the capacitance values of parametric elements are time functions. Taking these variables into account, a capacitance/voltage converter can be designed, the output voltage of which will give information necessary for control and stabilization of primary oscillations.

For linearization of the total electrostatic force, comb electrodes are actuated by a combination of DC and AC voltages. The schematic of the balance actuator of MMG sensor on the excitation axis is presented in Fig. 6.

The electrostatic analysis carried out for the MMG structure shows that capacitance $C13$ does not practically depend on the modal coordinate, so $I13 \approx 0$. The law of capacitance variation for $C1$ and $C2$ can be represented by:

$$\begin{aligned} C1(t) &= a + bx(t); \\ C2(t) &= a - bx(t), \end{aligned} \qquad (1)$$

where a, b are scaling factors; $x(t)$ is the law of motion.

The motion $x(t)$ of the MMG sensor on the axis of

primary oscillations that can be obtained from:

$$\frac{\partial^2 x}{\partial t^2}+\frac{\omega_x}{Q}\frac{\partial x}{\partial t}+\omega_x^2 x=\frac{1}{m_x}F_x(t), \quad (2)$$

where Q is the quality factor of the primary oscillation channel; $F_x(t)$ is the excitation force of primary oscillations.

We will find solution of the equations (2) at sinusoidal excitation force in the form:

$$x(t)=X_m\sin(\omega t+\varphi_0), \quad (3)$$

where X_m is the amplitude of sensor movement.

Then the primary oscillation amplitude and phase are determined by the following equations:

$$X_m=\frac{F_m}{m_x\sqrt{\left(\omega_x^2-\omega^2\right)^2+\frac{\omega_x^2\omega^2}{Q^2}}};$$
$$\varphi_0=-\arctan\frac{\omega_x\omega}{Q\left(\omega_x^2-\omega^2\right)}. \quad (4)$$

The electrostatic force is calculated as the derivative of the capacitance function:

$$F_x(t)=\frac{1}{2}\frac{\partial C_1(t)}{\partial x}U_1^2(t)+\frac{1}{2}\frac{\partial C_2(t)}{\partial x}U_2^2(t);$$
$$U_1(t)=U_0+U_m\sin(\omega t); \quad (5)$$
$$U_2(t)=U_0-U_m\sin(\omega t).$$

Substituting (1) in (5), we get:

$$F_x(t)=2bU_0U_m\sin(\omega t). \quad (6)$$

From (6), the amplitude of the primary oscillation excitation force does not depend on coordinate x(t) while the differential equation of the sensor motion on the axis of primary oscillations is linear under these conditions.

The amplitude of primary oscillations under at resonance is obtained from:

$$X_m=\frac{F_mQ}{m_x\omega_x\omega}=\frac{2bU_0U_mQ}{m_x\omega_x^2}, \quad (7)$$

then:

$$U_0U_m=\frac{X_m m_x\omega_x^2}{2bQ}. \quad (8)$$

Let us assume that $\omega_x = \omega$ and $U_0 = 10$ V, then the voltage U_m can be obtained at different quality factors (see Table 1).

Table 1. Voltage from quality factors

Q	10	100	200	500	1000
U_m (V)	162	16.2	8.1	3.24	1.62

The comb-drive actuator should be selected with regard for the energy relationships that provide the oscillation of inertial mass with the selected amplitude X_m.

IV. PRIMARY OSCILLATION CONTROL SYSTEM

Currents passing through capacitances $C1$ and $C2$ of the balance actuator can be obtained from:

$$I_{C1}(t)=\frac{\partial C1(t)}{\partial t}U_1(t)+\frac{\partial U_1(t)}{\partial t}C1(t)=$$
$$=\begin{pmatrix}bX_mU_m\sin(2\omega t+\varphi_0)+\\+bX_mU_0\cos(\omega t+\varphi_0)+U_m\cos(\omega t)\end{pmatrix}\omega,$$
$$I_{C2}(t)=\frac{\partial C2(t)}{\partial t}U_2(t)+\frac{\partial U_2(t)}{\partial t}C2(t)= \quad (9)$$
$$=\begin{pmatrix}bX_mU_m\sin(2\omega t+\varphi_0)-\\-bX_mU_0\cos(\omega t+\varphi_0)-U_m\cos(\omega t)\end{pmatrix}\omega.$$

The total current passing through capacitances can be obtained from:

$$I_C(t)=I_{C1}(t)+I_{C2}(t)=2b\omega U_mX_m\sin(2\omega t+\varphi_0). \quad (10)$$

Provided the resonance tuning of the primary oscillation channel $\omega_x = \omega$, $\varphi_0 = -90°$. In case of changing the resonant frequency, the angle $\varphi 0$ is changed also. To stabilize the primary oscillation frequency and achieve the amplitude close to its maximum, it is necessary to measure the in-phase and quadrature components of the current passing through one of the comb-drive actuator capacitances or 2ω frequency total current.

Stabilization of primary oscillations shown schematically in Fig. 7, is based on measurements of the total current that passes through the balance actuator capacitances.

Thanks to the properties of the Op-amp, the actuator capacitances are grounded to a virtual point (complemented input of the Op-amp) rather than connected with the ground. The in-phase and quadrature components of 2ω frequency current after the lock-in detection and filtering with a low-pass filter are obtained from

$$U_p=\lim_{T\to\infty}\frac{1}{E\cdot T}\int_0^T U_{I(t)}\cdot U_r\sin(2\omega t)dt=b\omega U_mX_m\cos(\varphi_0)$$
$$U_q=\lim_{T\to\infty}\frac{1}{E\cdot T}\int_0^T U_{I(t)}\cdot U_r\cos(2\omega t)dt=b\omega U_mX_m\sin(\varphi_0) \quad (11)$$

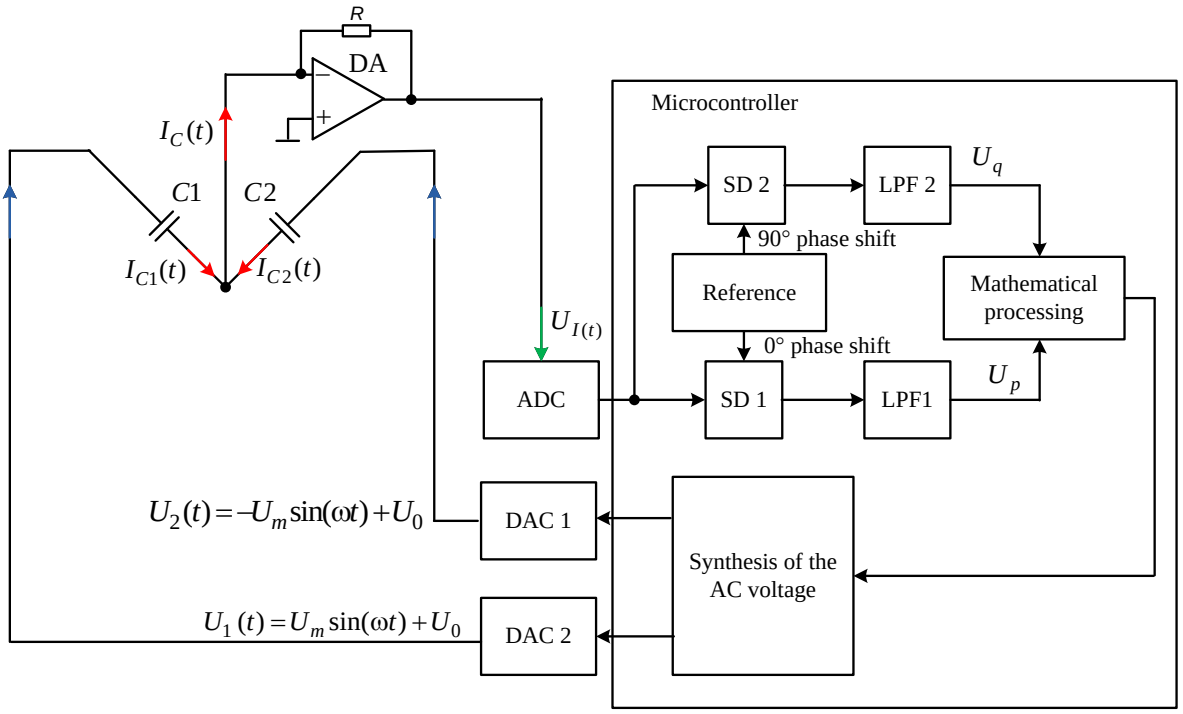

Fig. 7. Schematic of primary oscillation stabilization: ADC – analog-digital converter; DAC – digital-analog converter; SD - synchronous detector ; LPF – low-pass filter.

Then the amplitude and phase of the total current passing through the capacitances have the form:

$$I_C = \sqrt{U_p^2 + U_q^2} = 2bX_m U_m \omega, \tag{12}$$

$$\varphi_0 = \arctan\frac{U_q}{U_p} = \arctan\frac{\omega_x \omega}{Q\left(-\omega_x^2 + \omega^2\right)}, \tag{13}$$

Using (4)-(6), the resonant frequency of the primary oscillation channel can be obtained from

$$\omega_x = -\frac{\omega\left(1 + \sqrt{1 + 4Q^2 \tan\left(\varphi_0\right)^2}\right)}{2Q\tan\left(\varphi_0\right)}. \tag{14}$$

After the calculation of resonant frequency, the frequency of voltage suppliers is changed in one step.

The operating principle of the primary oscillation stabilization circuit with lock-in technique [18-19] shown in Fig. 7 is as follows. With MMG power on, microcontroller sets the initial frequency and amplitude of voltages U_1 and U_2 using the digital-analog converters DAC 1 and DAC 2. The analog-digital converter is then used to measure the total current, while using (11)-(14), we calculate the deviation of the set frequency from resonant frequency of the sensor. In case of over 0.1 % deviation, the frequency of voltages U_1 and U_2 is to be corrected.

V. NUMERICAL ANALYSIS OF PRIMARY OSCILLATION CONTROL SYSTEM

The numerical analysis is carried out assuming that U0 = 5 V and Um = 3,24 V; Q = 1000; b = 1,6737028·10-8 and ωx = 10 kHz. Then the maximum movement of the inertial mass Xm = 5·10-6 μm.

Fig. 8, and 9 present dependence curves of φ0 phase and amplitude of the total current at 2 % change of the MMG natural resonant frequency.

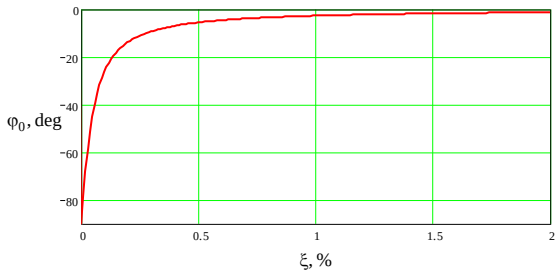

Fig. 8. Dependence between total current φ0 phase and natural resonant frequency

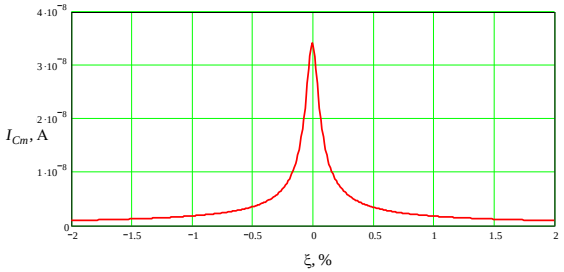

Fig. 9. Dependence between total current amplitude and natural resonant frequency

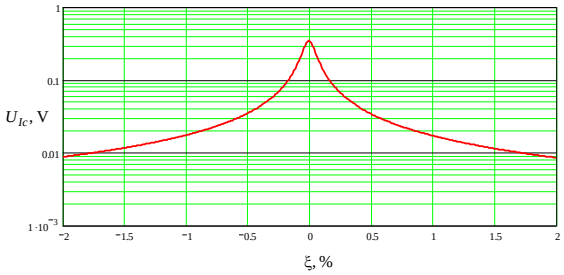

Fig. 10. Dependence between total current amplitude and natural resonant frequency

The plots contained in Fig. 8 and 9 show that the insignificant detuning of frequency results in significant change of the phase and the amplitude of the total current.

In case 10 MOhm resistor is placed in the feedback of Op-amp that converts the total current into voltage (Fig. 7), the dependence curve of this voltage amplitude depending on 2 % change of the MMG natural resonant frequency assumes the shape shown in Fig. 10.

According to Fig. 10, the voltage ranges from 500 mV (at frequency coincidence) to 9 mV (at 2 % difference of frequencies). Hence, the voltage digitization does not require the additional amplifiers between the current/voltage converter and a high resolution analog-digital converter. A simple ten-digit analog-digital converter with 2.56 V reference voltage will be enough after the current/voltage conversion. Actually, the use of a ten-digit analog-digital converter provides the minimum voltage of 2.5 mV.

VI. CONCLUSIONS

The primary oscillation control system was designed to provide the movement of inertial mass and the stabilization of primary oscillations in the two-component micromechanical gyroscope. The suggested approach allows optimization of the comb-drive actuator structure merely due to capacitances used for both excitation of primary oscillations and data retrieval for their stabilization.

The suggested method of calculating natural resonant frequency is based on measurements of the total current passing through the comb-driver actuator capacitances and the lock-in detection. This allowed tuning of the primary oscillation frequency in one-step frequency change of voltage suppliers and avoiding a long-term transition process typical for the traditional frequency stabilization circuits based on proportional-integral derivative controllers.

ACKNOWLEDGMENTS

This research was conducted in Tomsk Polytechnic University and financially supported by the Ministry of Education and Science of the Russian Federation (agreement No.14.575.21.0068, unique identifier RFMEFI57514X0068).

REFERENCES

[1] K. Liu, et al., “The development of micro-gyroscope technology”. J. Micromech. Microeng. 2009, vol. 19, pp. 1-29.

[2] M.N. Armenise, C. Ciminelli, F. Dell’Olio and V.M.N. Passaro, “Advances in Gyroscope Technologies,” Springer: Berlin/Heidelberg, Germany, 2011.

[3] H.K. Xie and G.K. Fedder, “Fabrication, characterization, and analysis of a DRIE CMOS-MEMS gyroscope,” IEEE Sens. J. 2003, vol.3, pp. 622–631.

[4] L. Aaltonen and K.A.I. Halonen, “An analog drive loop for a capacitive MEMS gyroscope,” Analog. Integr. Circuit Signal, 2010, vol. 63, pp. 465-476.

[5] W. Sung, et al., “Development of a lateral velocity-controlled MEMS vibratory gyroscope and its performance test,” J. Micromech. Microeng. 2008, vol.18, pp. 1-14.

[6] J. Cui, et al., “Transient response and stability of the AGC-PI closed-loop controlled MEMS vibratory gyroscopes,” J. Micromech. Microeng. 2009, vol. 12, pp. 1-17.

[7] J.C. Fang, J.L. Li, and W. Sheng, “Improved temperature error model of silicon MEMS gyroscope with inside frame driving”, J. Beijing Univ. Aeronautics Astron., vol. 32, pp. 1277-1280, Dec. 2006.

[8] R. Feng, A. P. Qiu, Q. Shi, and Y. Su, “A theoretical and experimental study on temperature dependent characteristics of silicon MEMS gyroscope drive mode,” Adv. Mater. Res., vols. 403–408, pp. 4237-4243, Nov. 2011.

[9] D. Xia, S. Chen, S. Wang, and H. Li, “Microgyroscope temperature effects and compensation-control methods,” Sensors, vol. 9, no. 10, pp. 8349-8376, Oct. 2009.

[10] S.-R. Chiu et al., “An integrated thermal compensation system for MEMS inertial sensors,” Sensors, vol. 14, no. 3, pp. 4290-4311, Mar. 2014.

[11] T.G. Nesterenko, A.N. Koleda, E.S. Barbin and S.V. Uchaikin, “Temperature Error Compensation in

Two-Component Microelectromechanical Gyroscope," in Components, Packaging and Manufacturing Technology, IEEE Transactions on, vol.4, no.10, pp. 1598-1605, Oct. 2014.

[12] D.Z. Xia, S.L. Chen and S.R. Wang, "Development of a prototype miniature silicon microgyroscope," Sensors 2009, vol. 9, pp. 4586-4605.

[13] B. Yang, B.L. Zhou and S.R. Wang, "A precision closed-loop driving scheme of silicon micromachined vibratory gyroscope". J. Phys. Conf. Series 2006, vol. 34, pp. 57-64.

[14] B. Yang, H.S. Li, B.L. Zhou and S.R. Wang, "Mechanical-thermal noise in drive-mode of a silicon micro-gyroscope," Sensors 2009, vol. 9, pp. 3357-3375.

[15] Bing Mo, Xiaowei Liu, Xuewei Ding and Xiaoyun Tan, "A Novel Closed-loop Drive Circuit for the Micromechined Gyroscope," in Mechatronics and Automation, 2007. ICMA 2007. International Conference on, pp. 3384-3389, 5-8 Aug. 2007.

[16] B. Eminoglu, S.E. Alper and T.Akin, "An optimized analog drive-mode controller for vibratory MEMS gyroscopes," Procedia Eng. 2011, vol. 25, pp. 1309-1312.

[17] Huan-ming Wu, Hai-gang Yang, Tao Yin and Hui Zhang, "Stability analysis of MEMS gyroscope drive loop based on CPPLL," in Microelectronics and Electronics (PrimeAsia), 2011 Asia Pacific Conference on Postgraduate Research, pp. 45-48, 6-7 Oct. 2011.

[18] P.F. Baranov, E.I. Tsimbalist, V.N. Borikov, and Soltanova D.G. "Measurement of the current transfer ratio for current shunts," in Proceedings of XXI IMEKO World Congress, 30 August-4 September. 2015.

[19] P.F. Baranov, E.I. Tsimbalist and V.E. Baranova "Instrument for measurement of transfer function voltage dividers," in Proceedings 2015 International Siberian Conference on Control and Communications (SIBCON), May 21-23, 2015.